Desalination and Water Treatment
www.deswater.com

doi:10.5004/dwt.2017.20196

66 (2017) 338–345
March

A nanohybrid of mixed ferrite—polyaniline derivative copolymer for efficient adsorption of lead ions: Design of experiment for optimal condition, kinetic and isotherm study

Hassan Alijani[a], Mostafa Hossein Beyki[b], Yousef Fazli[c,*], Zahra Shariatinia[a]

[a]*Department of Chemistry, Amirkabir University of Technology, Tehran, Iran, email: Alijani.hassan89@gmail.com (H. Alijani), shariati@aut.ac.ir (Z. Shariatinia)*
[b]*School of Chemistry, University College of Science, University of Tehran, Tehran, Iran, email: hosseinbakim@gmail.com (M.H. Beyki)*
[c]*Department of Chemistry, Faculty of Science, Arak Branch, Islamic Azad University, Arak, Iran, Tel./Fax +98 86 33670017, email: y-fazli@iau-arak.ac.ir (Y. Fazli)*

Received 15 April 2016; Accepted 24 August 2016

ABSTRACT

In this work magnetic polymer nanocomposite was synthesized based on organic acid immobilized $MnMgFe_2O_4$ mixed ferrite. For this purpose, magnetic ferrite was prepared through precipitation and calcining at 700°C. After that, the ferrite was further reacted with (3- chloropropyl) triethoxysilane and amino sulfonic acid. Modified magnetic material was applied for preparing copolymer with phenylenediamine. Magnetic polymer nanocomposite was characterized using FT–IR, EDX, XRD, SEM, TEM, VSM, and TGA techniques. Moreover, the nanocomposite was employed as a magnetic recyclable adsorbent for adsorption of lead ions from aqueous solutions. Optimal conditions have been obtained with Box-Behnken design (BBD). Equilibrium was achieved within 10 min and adsorption followed second order kinetic model. Isotherm study revealed that magnetic nanocomposite has maximum adsorption capacity of 330 mg g^{-1} and Freundlich model goodly describe adsorption behavior of the sorbent. Adsorbed ions were released with HNO_3 solution (0.1 mol L^{-1}) and the sorbent showed good adsorption efficiency after 3 cycle of sorption and desorption.

Keywords: Design expert; Ferrite; Lead; Nanocomposite; Polymer.

1. Introduction

Pollution of heavy metals is a major environmental threat since bio-accumulation of them cause serious ecological and health hazards [1,2]. Among heavy metals, lead is a nonessential, highly toxic metal as exposure on excess of it cause severe damage to brain, nervous system and may cause neonatal death [3,6]. Some of widely applied lead separation methods include: membrane filtration [7], coprecipitation [8], solid phase extraction (SPE) [9,10], gravitational settling—sedimentation [11] and liquid–liquid extraction [12]. Due to high efficiency and low consumption of pure organic solvents, adsorption methods attracted a considerable amount of interest for the adsorption of toxic metal ions. Choosing an appropriate adsorbent is a key factor in the mentioned methods, since this factor could affect selectivity and sensitivity of the adsorption process [13,14]. Due to significance of adsorption, various sorbents have been proposed such as; carbon nanotubes [15,17] nano alumina [18] resin [19,20] nanoclay [21], biosorbents [22,23], graphene [24], polymeric adsorbent [25,27] and magnetic nanoparticles [28,29]. Among these sorbents, magnetic nanoparticles (MNPs) and their nanocomposites have gained great deal of attentions owing to their homogenous dispersion in the solution phase and ability to control and separate them by an external magnetic field [30,31]. The most conventional MNPs used directly as adsorbents or supports in separation procedure are iron oxides comprised nanoparticles

*Corresponding author.

and spinel ferrites with MFe_2O_4 formula (M: Mn, Co, Cu, Ni, Ca, Zn), as the later have been widely investigated for their high magnetic permeability and chemical stability [32,33]. However, aggregation and changes of surface properties limited direct application of nanoparticles in adsorption methods. One of the most notable candidates for improvement of such practical applications may be magnetic polymer nanocomposite. In fact, combine the magnetic properties with the polymer characteristics creat a suitable protective layer which cause unique and tailored properties along with reliable chemical stability. Furthermore, polymer functional groups can provide a robust platform for sensing application as well as increases selectivity and sensitivity of adsorption methods for target species [34,35]. To date, a number of polymer nanocomposites have been used for heavy metal adsorption. Polyaniline derivative is one of the convenient materials with many features, which could be exploited in various applications [36]. Polyaniline derivative has high content of functional groups in conjugated structure and more intriguing multi-functionality such as –OH, $–NH_2$ and $–SO_3$ which increase adsorption capacity. Powerful chelation ability as well as the accessibility of the functional groups reduces diffusion resistant which causes low equilibrium time and fast adsorption process. However, polyaniline derivatives have small specific surface area which restricts its application for metal adsorption. This limitation can be improved by polymer combination with magnetic nanoparticles [37]. Moreover, magnetic polymer can be easily separated from solution by simple external magnetic field.

The goal of this study is exhibit a novel magnetic polymer nanocomposite for lead adsorption. For this purpose, $MnMgFe_2O_4$ mixed ferrite was synthesized and modified with amino sulfonic acid. The organic acid acts as a monomer, which can be condensed with p-phenylenediamine as basic monomer hence, the yield of polymerization reaction is a copolymer that chemically attached to nanoparticles surface. Prepared magnetic nanocomposite was applied as a magnetic recyclable adsorbent for lead adsorption from aqueous solutions. Effective parameters on adsorption process were optimized with Box-Behnken design (BBD). Kinetic and isotherm models were also studied.

2. Experimental section

2.1. Materials and instruments

All reagents i.e, $Fe(NO_3)_3{\cdot}9H_2O$, $Mn(NO_3)_2{\cdot}4H_2O$, $Mg(NO_3)_2$, and NaOH were analytical grade and used as received without further purification. (3-chloropropyl) triethoxysilane (CPTES), 4-amino–benzene sulfonic acid, 1,4–phenylenediamine, sodium thiosulfate ($Na_2S_2O_3$) and sodium dodecyl sulfate (SDS) supplied from Merck (Darmstadt, Germany). Standard solution of Pb(II) ions (1000 mg L^{-1}) was prepared with dissolving of Pb $(NO_3)_2$ salts (Merck product) in a minimum amount of HNO_3, and then diluted to appropriate volume with distilled water. The pH adjustment was performed with 0.1 mol L^{-1} of HNO_3 and 0.1 mol L^{-1} of NH_3.

The prepared particles were characterized by powder X-ray diffraction analysis using a Phillips powder diffractometer, X′ Pert MPD, with Cu-Ka (λ = 1.540589 Å) radiation in 2θ range of 2–100˚. Fourier transform infrared spectra (FT-IR) were measured with Equinox 55 Bruker with ATR method over the wavelength of 400–4000 cm^{-1}. TEM and FE-SEM analysis carried out using Zeiss-EM10C and HITACHI S 4160 instruments, respectively. TGA results and energy dispersive X-ray spectrometry (EDX) are recorded with a TA- Q-50 and Oxford ED-2000 (England) respectively. A Varian model AA- 400 flame atomic absorption (FAAS) spectrometer (Varian Australia Pty Ltd, Musgrave), equipped with a deuterium lamp background and hollow cathode lamp was used for determination of lead ions. A digital pH-meter (model 692, metrohm, Herisau, Switzerland), was used for the pH adjustment.

2.2. Preparation of modified ferrite

For synthesis of the $MnMgFe_2O_4$ NPs, 3.8 g of iron nitrate, 0.47 g of manganese nitrate and 0.72 g of magnesium nitrate, were dissolved in 100 mL of distilled water, and 50 mL of sodium hydroxide solution (2.0 mol L^{-1}) was added to metal solution along with vigorous stirring for 5.0 min. After that the precipitate was collected with filter paper, washed with distilled water, dried at 100˚C for 1 h, and further heated at 700°C for 1.5 h. To immobilize the organic acid on the surface of NPs, 1.0 g of ferrite was refluxed in 30 mL of methanol (containing 2 mL of CPTES and 0.5 g of the amino sulfonic acid) for 24 h. Then, the product was collected with external magnetic field and rinsed with methanol and dried at 60°C for 5 h.

2.3. Preparation of polymer nanocomposite

About 0.5 g of the modified nanoparticles was ultrasonically dispersed in SDS solution (1.5 g in 50 mL distilled water) for 10 min then, 1.0 g of 1,4 phenylenediamine was added to this mixture. After dropping of thiosulfate solution (1.5 g in 20 mL distilled water), the mixture was stirred for 24 h at room temperature. Obtained black precipitate was washed three times with HCl solution (0.1 mol L^{-1}) and several times with distilled water and dried at 80°C for 5 h. The process of magnetic nanocomposite preparation is schematically illustrated in Fig. 1.

2.4. Metal adsorption experiment

Metal adsorption experiments were performed for different concentrations of lead ions (0.05–50 mg L^{-1}) through batch method. For this purpose the pH of lead solutions in 50 mL volumetric flasks, were adjusted in 6.0 then, 10 mg of magnetic polymer was added to each flask. After shaking for 10 min, the concentration of lead ions in supernatant or in 5 mL of HNO_3 (0.1 mol L^{-1}) as eluent, was determined by FAAS. The same procedure performed for all blank solutions.

3. Results and discussion

3.1. Characterization of magnetic nanocomposite

The result for EDX analysis (Fig. 2a) exhibits the weight ratios of Fe (57.5%), O (19.3%), Mn (11.9%), Mg

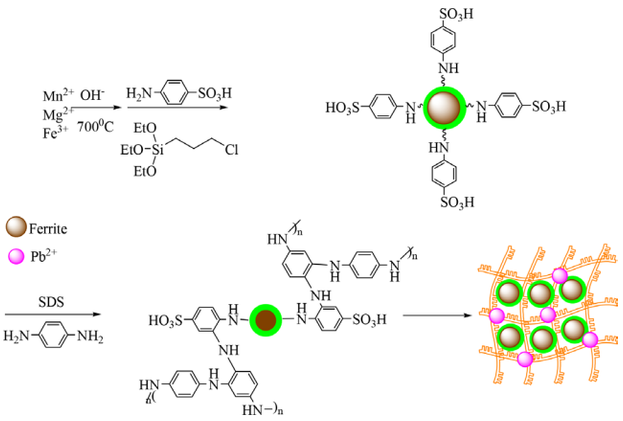

Fig. 1. The process of magnetic nanocomposite preparation.

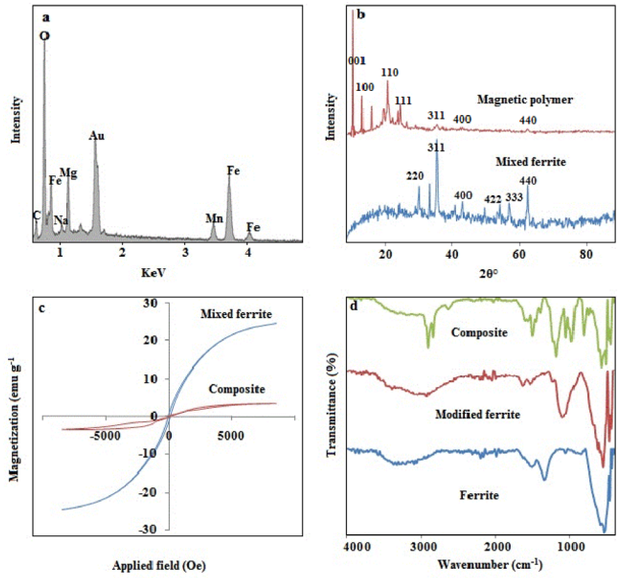

Fig. 2. EDX spectra (a), XRD pattern (b), VSM graph (c) and FT-IR spectra (d) for prepared composite.

(6.1%), C (4.4%) and Na (0.9%). The XRD analysis of mixed ferrite and polymer nanocomposite are shown at Fig. 2b. The characteristic peaks due to ferrite crystal shows scattering at 2θ° = 30.9, 35.34, 40.76, 43.0, 53.52, 57.48 and 62.3 indexed to the (220), (311), (400), (422), (333), and (440) planes of a cubic cell. The result matched with the spectra of both $MnFe_2O_4$ (JCPDS-74-2403) and $MgFe_2O_4$ (JCPDS 73-2410) which prove formation of mixed ferrite. Polymer nanocomposite exhibits new peaks at 2θ° = 10.12, 15.49, 20.26 and 24.0 due to crystallinity of (001), (100), (110) and (111) planes [38,40]. Magnetic hysteresis loops of prepared NPs and polymer (Fig. 2c) showed the saturated magnetization of 24.5 and 3.45 emu g^{-1} respectively. The quench in the magnetic moment for polymer nanocomposite is due to the existence of organic layers on the surface of magnetic core.

In the FT-IR spectra of naked and modified ferrite at Fig. 2d, the characteristic bands of Fe–O (569 cm^{-1}), vibration of Mg–O and Mn–O (600–1000 cm^{-1}), stretching vibration of Si–O (1100 cm^{-1}) and C–H stretching (2929 cm^{-1}) are observable. The spectra of polymer nanocomposite show peaks at 2919 cm^{-1}, 1571 cm^{-1} and 1400–1500 cm^{-1}, which assigned to C–H stretching, N–H bending units and aromatic backbone vibration, respectively.

The FE-SEM image of ferrite is shown in Fig. 3a. Synthesized materials are spherical clusters with diameter in the range of 40 to 60 nm. In fact the discrete nanoparticles are not observable. Cluster formation is owing to the interaction between the particles with high surface activity through hydrogen bonding. Due to the crosslinking between polymer fragments, the image of polymer composite (Fig. 3b) present irregular flakes. The TEM image of polymer nanocomposites (Fig. 3c), exhibits distribution of magnetic nanoparticles as dark points in polymer matrices. After composite formations the polymer can acts as spacer between the particles and destroy the clusters structure hence it can be seen that diameter of ferrite nanoparticles is less than 10 nm.

Thermal gravimetric analysis for polymer nanocomposite is shown in Fig. 3d. The result shows that the total weight loses over the temperature range of 50-600°C is about 75% for polymer nanocomposite. Polymer nanocomposite underwent three stages of weight loss owing to the release of water and chain decomposition at elevated temperature. The first weight loss has been observed below 100°C, which may be attributed to the loss of volatilized moisture. The second weight loss which was below 200°C may be attributed to the re-crystallization, and crosslinking reactions of the polymer chains. At more extreme temperatures, other main weight loss has been occurred around 250, 300 and 400–530°C due to polymer backbone degradation. This result confirms that polymer has been synthesized on the surface of ferrite with high density.

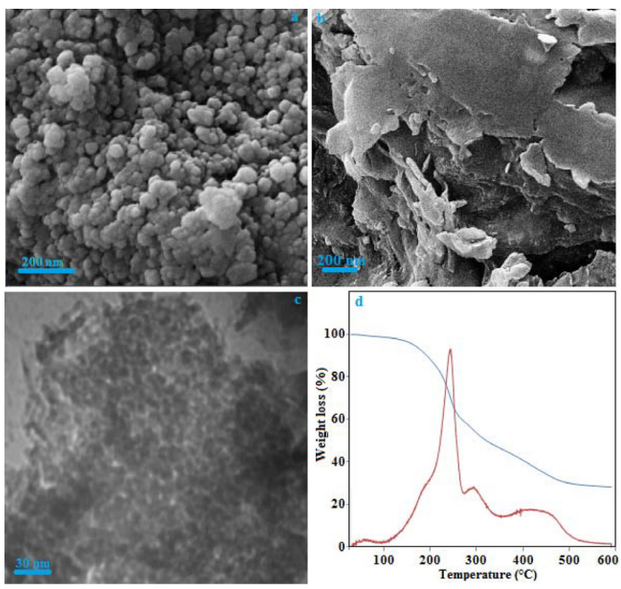

Fig. 3. FE-SEM image of the ferrite and polymer nanocomposite (a and b), TEM image of polymer nanocomposite (c), and TGA – DTA graph for polymer nanocomposite (d).

3.2. Optimization of sorption process using response surface methodology

Box–Behnken design (BBD) was adopted for studying the adsorption of Pb(II) by the magnetic nanocomposite. Three significant parameters namely pH (A), adsorption time (B) and adsorbent dosage (C) was optimized. Owing to use of three variables, 17 experimental runs were required. A quadratic model was performed between the response and the corresponding coded values and finally, the best fitted model equation was obtained as:

$$\%R = 99.85 + 1.0A + 1.0B + 0.7C + 0.7AB + 0.2AC + 0.2BC - 3.0A^2 - 1.0B^2 - 1.6C^2 \quad (1)$$

The statistical significance of the equation was evaluated by the analysis of variance (ANOVA). According to results, the P-value (<0.0001) is lower than 0.05 indicating that quadratic model was significant. The low value of standard deviation (0.5) between the experimental and predicted results shows that Eq. (1) adequately represents actual relationship between the response and significant variables. High value of R^2 (0.98) and adjusted R^2 (0.95) indicates a high dependence and correlation between the observed and the predicted values of response. Adequate precision measures the signal to noise ratio and a ratio of 15.7 was obtained for adsorption efficiency which demonstrated that model is significant for the process. The 3D response surface plots for the removal percentage (R%) were shown in Fig. 4. The results showed that the best pH is 6 as well as optimum contact time and adsorbent dosage were 10 min and 10 mg, respectively.

3.3. Kinetic study

Quantifying the changes in adsorption with time can be investigated using the appropriate kinetic model. The pseudo-first-order and pseudo-second-order model can be expressed by following equations.

$$\ln(Q_e - Q_t) = \ln Q_e - k_1 t \quad (2)$$

$$\frac{t}{Q_t} = \frac{1}{(K_2 Q_e^2)} + \left(\frac{1}{Q_e}\right) t \quad (3)$$

where k_1, k_2, Q_e and Q_t are the pseudo-first order adsorption rate constant (min^{-1}), the second-order rate constant (g mg^{-1} min^{-1}) and the values of the amount adsorbed per unit mass at equilibrium and at any time t respectively [41]. The plots of second order model showed better linearity respect to first order (Fig. 5a and 5b). Moreover, according to results in Table 1, the Q_e correspond to the second-order model has low deviation (0.72 %) from experimental value hence, chemical adsorption based of second order model can be accepted as the mechanism for lead adsorption.

The intra-particle diffusion model describes transport of analyte from the aqueous phase to the surface of the adsorbent and subsequent diffuse into the interior of the particles [42]. This model can be presented by the following equation:

$$Q_t = k_i t^{0.5} + C \quad (4)$$

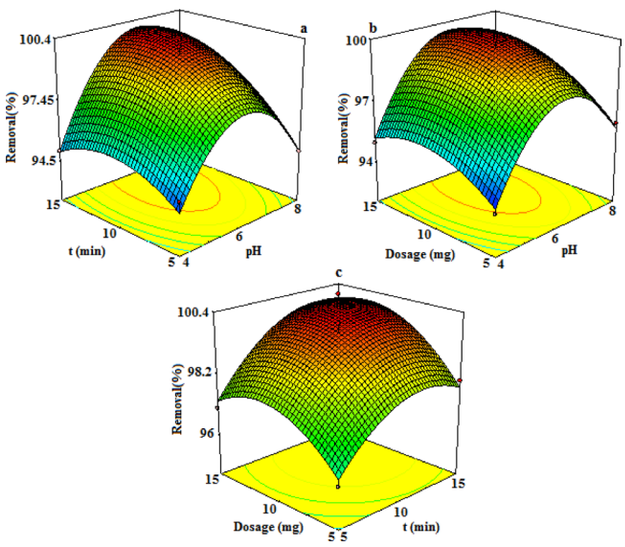

Fig. 4. Estimated response surface by plotting removal percentage (R%) versus pH–adsorption time (a), pH–adsorbent dosage (b) and time–adsorbent dosage (c).

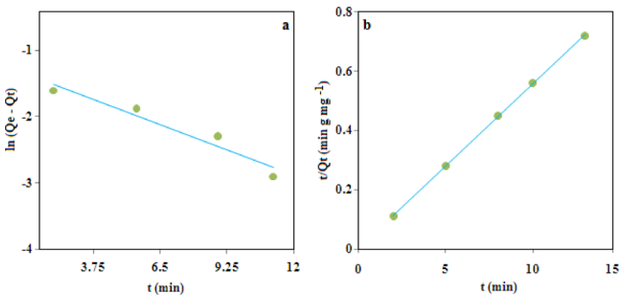

Fig. 5. Lagergren pseudo-first order (a) and second order (b) kinetic model for lead adsorption.

Table 1
The data of kinetic models for adsorption of Pb^{2+} ions using polymer nanocomposite

	R^2	0.939		R^2	0.955
First order	K_1	0.15	Diffusion model	K_i	0.88
	Q	0.3		C	14.86
	R^2	0.999		R^2	0.782
Second order	K_2	3.03	Liquid film	K_{fd}	0.24
	Q	18.18		C	1.55
				R^2	0.94
			Elovich	α	2.9×10^6
	Q_{exp}	18.05		β	0.97

The plot of Q_t versus $t^{0.5}$ (Fig. 6a), is approximately linear with an intercept of 14.86 instead of zero hence, this model unlikely to be rate controlling.

The liquid film diffusion model (Eq. (5)) explains the role of transport of the analyte from the liquid phase up to the boundary of solid phase.

$$ln\left(1-\frac{Q_t}{Q_e}\right)=k_{fd}t+C \tag{5}$$

where k_{fd} is the adsorption rate constant [43]. The curve of this model (Fig. 6b) is not linear moreover, it has the intercept of 1.55 against the predictions of the model consequently, and this model cannot be accepted as kinetic mechanism.

The Elovich kinetic model can be expressed as:

$$Q_t=\frac{1}{\beta}\,ln(\alpha\beta)+\frac{1}{\beta}\,ln(t) \tag{6}$$

which α (mg g^{-1} min^{-1}) and β (g mg^{-1}) represent the initial adsorption rate and desorption constant respectively. The plot of Q_t vs. ln (*t*) (Fig. 6c) is linear with high value of α, which confirm high adsorption rate and good affinity of lead ions toward the polymer nanocomposite.

3.4. Isotherm study and error analysis

The equilibrium adsorption isotherm can describe the mechanism of sorbate–adsorbent interaction hence, the effect of Pb(II) concentration on adsorption process was analyzed in terms of Freundlich and Langmuir isotherms. The Freundlich model is represented as:

$$\ln Qe=\ln K_f+\left(\frac{1}{n}\right)\ln Ce \tag{7}$$

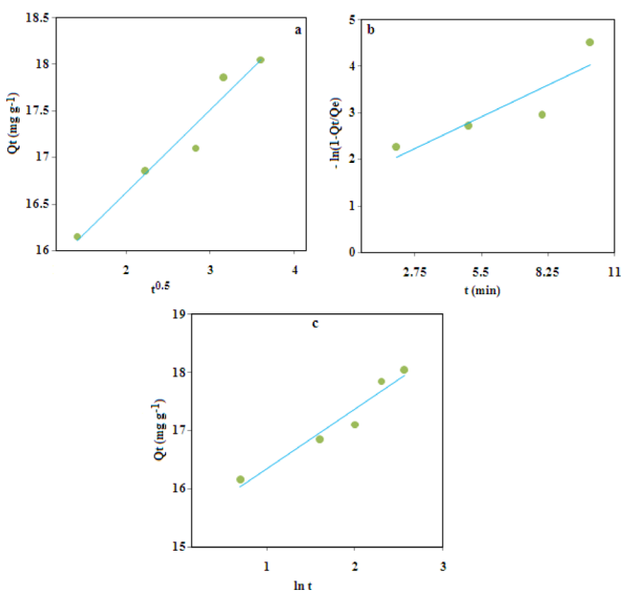

Fig. 6. Intra-particle diffusion (a), liquid film diffusion (b) and Elovich model (c) for lead adsorption using the polymer nanocomposite.

where *n* and K_f are the Freundlich coefficients which evaluated from the slope and intercept of linear plot. Q_e is the amount of metal ions sorbed per unit mass of the sorbent (mg g^{-1}) and C_e (mg L^{-1}) is the amount of metal ions in the liquid phase at equilibrium [44].

Linear form of Langmuir model can be expressed by following equation:

$$\frac{C_e}{Q_e}=\frac{1}{Q_m}b+\frac{C_e}{Q_m} \tag{8}$$

The Q_m is maximum adsorption capacity and *b* is the Langmuir coefficient [45,47]. The essential characteristics of the Langmuir isotherm can be explained in terms of a dimensionless constant separation factor (R_L), calculated by use of the following equation:

$$R_L=\frac{1}{(1+bC_i)} \tag{9}$$

where C_i is the initial concentration of metal ions and R_L describes the type of Langmuir isotherm, to be unfavorable (R_L > 1), linear (R_L = 1), irreversible (R_L = 0) or favorable (0 < R_L < 1). The graphs for linear and nonlinear isotherm model are depicted in Fig. 7a–c, and results are listed in Table 2 which revealed that the nanocomposite has good adsorption efficiency as maximum adsorption capacity of the sorbent is 330 mg g^{-1}. Furthermore, R_L value was in the range of 0.17–0.67 which confirm Langmuir model is favorable for lead adsorption using the magnetic nanocomposite. To evaluate the accuracy and fitness of isotherm model with experimental results, the coefficient of determination (r^2) and the chi-square test (χ^2) were used in this study. These error functions are given as:

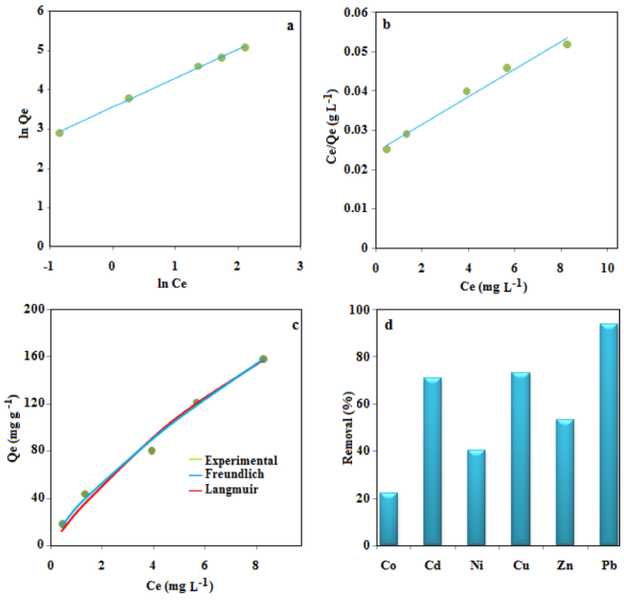

Fig. 7. Freundlich and Langmuir adsorption isotherm models (a and b), the theoretical isotherm model fitted with experimental data (c), and removal efficiency of some heavy metals using the polymer nanocomposite (d).

Table 2
The data of isotherm models for lead adsorption using magnetic polymer nanocomposite

Langmuir	Value	Freundlich	Value
Q_m(mg g^{-1})	330	K_f	34.29
R^2	0.982	R^2	0.998
b	0.12	n	1.35
R_L	0.17 - 0.67	r^2	0.991
r^2	0.985	χ^2	0.095
χ^2	0.164		

$$r^2 = \frac{\Sigma\left(Q_c - \bar{Q}_{exp}\right)^2}{\Sigma\left(Q_c - \bar{Q}_{exp}\right)^2 + \Sigma\left(Q_c - Q_{exp}\right)^2} \quad (10)$$

$$\chi^2 = \Sigma\frac{\left(Q_{exp} - Q_c\right)^2}{Q_c} \quad (11)$$

where Q_{exp} and Q_c (mg g^{-1}) are the experimental adsorption capacity and the calculated from nonlinear models and $\bar{Q}_{exp}$ is average of Q_{exp} [48]. According to the results (Table 2), the value of R^2 for both linear models are superior to 0.90, indicate the low variance around the mean values. But, the Freundlich model have higher coefficient of determination and lover χ^2 value which confirmed that adsorption-complexation reactions taking place in the adsorption process. Moreover, the value of error analysis for Langmuir model are close to Freundlich model hence, the model show good fitness due to homogeneous distribution of active sites on the sorbent. It is well known that the Langmuir isotherm corresponds to a dominant ion exchange mechanism these indicate that the mechanism of lead adsorption is complex and both the chemical adsorption and physical adsorption exist at the same times in this adsorption process. In other words, the sorbent possess both heterogeneous and homogeneous active sites which interact with target ions. Moreover it can estimate that adsorption occur through monolayer chemisorption followed with multilayer physisorption process.

3.5. Specificity of the method

To investigate the specificity of the nanocomposite toward lead ions the procedure was performed for different metal solution with concentration of 2 mg L^{-1} for nickel, cobalt, copper, cadmium, and zinc ions. The result (Fig. 7d) indicated that the removal efficiency at optimum conditions are more than 90% for lead ions but for other ions is in the range of 50–70% that shows the efficiency of method for lead adsorption.

Ions become specifically adsorbed when short-range interactions between them and the interphase become important. They are believed then to penetrate into the inner layer and may come into contact with the surface. It is known that affinity of coordination sites toward a species can be owing to overlapping between bonding orbital's of the species involved in the reaction as well as matching of pore mouth diameter with molecular size of fed species. Good specificity of the sorbent toward lead ions confirms that there is a strong solid–fluid phase interactions between the lead ions and the adsorbent surface. In fact tightly bound Pb– polymer is considered to form a rigid structure which does not change in the course of charge transfer. Moreover, it estimates that the size of pores is more matched with lead ions which facilitate its diffusion through adsorbent pores [49,51].

3.6. Regeneration of the sorbent

Regeneration of solid sorbent is a prominent epithet based on economic view hence, release of adsorbed lead ions from sorbent surface was also investigated. According to effect of pH on lead adsorption, the removal efficiency was not quantitative in acidic situations therefore; it can be estimated that acidic solution may be good eluent for Pb desorption. As a result, different concentration of HNO_3 solution was applied and the result showed that the solution with concentration of 0.1 mol L^{-1} can release target ions with efficiency of 95%. To evaluate the reusability of the sorbent, it was washed with water then dispersed in 50 mL of lead solution, the pH was adjusted at 6 and the general adsorption procedure was performed. It was observed that after 3 cycle of sorption and desorption the removal efficiency was more than 90% which indicate the sorbent has good potential to be applied as a recyclable adsorbent.

3.7. Comparison with the literature

The performances of proposed method for Pb^{2+} adsorption have been compared with some literature and results are depicted in Table 3. It is obvious that this method has better performance relative to most previous ones with respect to the adsorption time; furthermore it shows satisfactory adsorption capacity. Prepared sorbent composed of mixed metal oxide i.e, MnO, MgO, and Fe_2O_3 as well as polymer fragment with various functional groups. In fact polymer active sites which including $–NH_2$ and $–SO_3H$ along with metal oxides are easily accessible to capture lead ions. Lead ions interact with these functional groups through ion exchange especially with $–SO_3H$, $–NH_3^+$ and $– OH_2^+$. Moreover, formation of inner sphere complex on the sorbent surface is another main mechanism which caused high efficiency of the sorbent for lead adsorption. Adsorption mechanism can be expressed as follow (Eqs. (12)–(15)).

$$–SO_3^-H^+ + Pb^{2+} \rightarrow –SO_3^-Pb^{2+} + H^+ \quad (12)$$

$$–NH_3^+ + Pb^{2+} \rightarrow –NH_2Pb^{2+} + H^+ \quad (13)$$

$$–NH_2 + Pb^{2+} \rightarrow –NH_2 – Pb \quad (14)$$

$$–SO_3H + Pb^{2+} \rightarrow –SO_3H – Pb \quad (15)$$

Table 3
Comparison the lead adsorption property of prepared material with some sorbents

Adsorbent	Maximum capacity (mg g^{-1})	Equilibrium time (min)	Ref
Banana peel	41.44	20	[2]
Rice bran	68	40	[3]
Chitosan nanofiber	577	8h	[4]
4-Aminoazobenzene - MWCNTs	46.8	10	[6]
Nanoporous silica	208	25	[13]
Pectin-based biosorbent	165	24h	[22]
Hydrilla verticillata biosorbent	125	120	[23]
Ion-imprinted polymer	75.4	5	[27]
O2-plasma-oxidized -MWCNTs	54.1	400	[41]
Cedar leaf ash	7.23	30	[46]
Graphene oxides	125	6h	[47]
MnMg Fe_2O_4 - Polymer	330	10	This work

4. Conclusions

A novel magnetic polymer nanocomposite have been demonstrated based on the chemically attachment of amino–sulfonic acid on mixed ferrite surface. Lead adsorption properties of the material were also investigated and optimized by design of experiment. The nanocomposite shows relatively fast adsorption kinetic for Pb^{2+} ions with high adsorption capacity and good reusability. The performance of this method was good with respect to efficiency and adsorption capacity and shows the ability of the method as an efficient adsorbent in order to solidify lead ions from aqueous solutions.

Acknowledgment

Support of this study by the research council of Islamic Azad University, Arak Branch, through grant is gratefully acknowledged.

References

[1] T. Sangvanich, J. Morry, C. Fox, W. Ngamcherdtrakul, S. Goodyear, D. Castro, G.E. Fryxell, R.S. Addleman, A.O. Summers, W.W. Yantasee, Novel oral detoxification of mercury, cadmium, and lead with thiol-modified nanoporous silica, ACS Appl. Mater. Interfaces, 6 (2014) 5483–5493.
[2] R.S.D. Castro, L. Caetano, G. Ferreira, P.M. Padilha, M.J. Saeki, L.F. Zara, M.A.U. Martines, G.R. Castro, Banana peel applied to the solid phase extraction of copper and lead from river water: preconcentration of metal ions with a fruit waste, Ind. Eng. Chem. Res., 50 (2011) 3446–3451.
[3] Y. Chen, L. Ding, J. Nie, Isotherm and thermodynamic studies of the biosorption of lead, cadmium and copper from aqueous solutions by rice bran, Desal. Water Treat., 44 (2012) 168–173.
[4] Y. Li, T. Qiu, X. Xu, Preparation of lead-ion imprinted crosslinked electro-spun chitosan nanofiber mats and application in lead ions removal from aqueous solutions, Europ. Polym. J., 49 (2013) 1487–1494.
[5] R.E. Green, D.J. Pain, Potential health risks to adults and children in the UK from exposure to dietary lead in game birds shot with lead ammunition, Food Chem. Toxic., 50 (2012) 4180–4190.
[6] Z. Li, L. Wu, Synthesis, characterization and application of 4-aminoazobenzene functionalized multiwalled carbon nanotubes as a novel and uniquely selective solid-phase extraction for determination of lead(II) in water samples, Intern. J. Environ. Anal. Chem., 94 (2014) 291–303.
[7] M. Soylak, Y.E. Unsal, N. Kizil, A. Aydin, Utilization of membrane filtration for preconcentration and determination of Cu(II) and Pb(II) in food, water and geological samples by atomic absorption spectrometry, Food Chem. Toxic., 48 (2010) 517–521.
[8] M. Soylak, A. Aydin, Determination of some heavy metals in food and environmental samples by flame atomic absorption spectrometry after coprecipitation, Food Chem. Toxic., 49 (2011) 1242–1248.
[9] S.G. Ozcan, N. Satiroglu, M. Soylak, Column solid phase extraction of iron(III), copper(II), manganese(II) and lead(II) ions food and water samples on multi-walled carbon nanotubes, Food Chem. Toxic., 48 (2010) 2401–2406.
[10] C. Er, B.F. Senkal, M. Yaman, determination of lead in milk and yoghurt by solid phase extraction using a novel aminothioazole – polymeris resin, Food Chem., 137 (2013) 55–61.
[11] F. Kaczala, M. Marques, W. Hogland, Lead and vanadium removal from a real industrial wastewater by gravitational settling/sedimentation and sorption onto pinus sylvestris sawdust, Biores. Technol., 100 (2009) 235–243.
[12] I. Komjarova, R. Blust, Comparison of liquid–liquid extraction, solid-phase extraction and co-precipitation preconcentration methods for the determination of cadmium, copper, nickel, lead and zinc in seawater, Anal. Chim. Acta, 576 (2006) 221–228.
[13] M. Behbahani, M. Salarian, M.M. Amini, O. Sadeghi, A. Bagheri, S. Bagheri, Application of a new functionalized nanoporous silica for simultaneous trace separation and determination of Cd(II), Cu(II), Ni(II), and Pb(II) in food and agricultural products, Food Anal. Methods, 6 (2013) 1320–1329.
[14] M. Ghaedi, K. Niknam, A. Shokrollahi, E. Niknam, H.R. Rajabi, M. Soylak, Flame atomic absorption spectrometric determination of trace amounts of heavy metal ions after Solid phase extraction using modified sodium dodecyl sulfate coated on alumina, J. Hazard. Mater., 155 (2008) 121–127.
[15] M. Soylak, Z. Topalak, Multiwalled carbon nanotube impregnated with tartrazine: solid phase extractant for Cd(II) and Pb(II), J. Ind. Eng. Chem., 20 (2014) 581–585.
[16] M. Tuzen, K.O. Saygi, M. Soylak, Solid phase extraction of heavy metal ions in environmental samples on multiwalled carbon nanotubes, J. Hazard. Mater., 152 (2008) 632–639.
[17] S.Z. Mohammadi, D. Afzali, D. Pourtalebi, Flame atomic absorption spectrometric determination of trace amounts of lead, cadmium and nickel in different matrixes after solid phase extraction on modified multiwalled carbon nanotubes, Cent. Eur. J. Chem., 3 (2010) 662–668.
[18] M. Medina, J. Tapia, S. Pacheco, M. Espinosa, R. Rodriguez, adsorption of lead ions in aqueous solution using silica–alumina nanoparticles, J. Non-Crystal. Solids, 356 (2010) 383–387.
[19] S. Tokalıoglu, A. Papak, S. Kartal, Separation/preconcentration of trace Pb(II) and Cd(II) with 2-mercaptobenzothiazole impregnated amberlite XAD-1180 resin and their determination by flame atomic absorption spectrometry, Arabian J. Chem. (2013) doi:10.1016/j.arabjc.2013.04.-017.
[20] A. Islam, A. Ahmad, M.A. Laskar, Preparation, characterization of a novel chelating resin functionalized with o-hydroxybenzamide and its application for preconcentration of trace metal ions, Clean – Soil, Air, Water, 40 (2012) 54–65.

[21] R. Rojas, Copper, lead and cadmium removal by Ca Al layered double hydroxides, Appl. Clay Sci., 87 (2014) 254–259.
[22] A. Jakóbik-Kolon, A.K. Milewski, K. Mitko, A. Lis, Preparation of pectin-based biosorbents for cadmium and lead ions removal, Sep. Sci. Technol., 49 (2014) 1679–1688.
[23] P.K.D. Chathuranga, D.M.R.E.A. Dissanayake, N. Priyantha, S.S. Iqbal, M.C.M. Iqbal, Biosorption and desorption of lead(II) by hydrilla verticillata, Biorem. J., 18 (2014) 192–203.
[24] Z.H. Huang, X. Zheng, W. Lv, M. Wang, Q.H. Yang, F. Kang, Adsorption of lead(II) ions from aqueous solution on low-temperature exfoliated graphene nanosheets, Langmuir, 27 (2011) 7558–7562.
[25] L. Wang, M. Zhou, Z. Jing, A. Zhong, Selective separation of lead from aqueous solution with a novel Pb(II) surface ion-imprinted sol-gel sorbent, Microchim Acta, 165 (2009) 367–372.
[26] L. Jin, R. Bai, Mechanisms of lead adsorption on chitosan/PVA hydrogel beads. Langmuir, 18 (2002) 9765–9770.
[27] M. Behbahani, A. Bagheri, M. Taghizadeh, M. Salarian, O. Sadeghi, L. Adlnasab, K. Jalali, Synthesis and characterisation of nano structure lead (II) ion-imprinted polymer as a new sorbent for selective extraction and preconcentration of ultra trace amounts of lead ions from vegetables, rice, and fish samples. Food Chem., 138 (2013) 2050–2056.
[28] C.Y. Cao, J. Qu, W.S. Yan, J.F. Zhu, Z.Y. Wu, W. G. Song, Low-cost synthesis of flowerlike α-Fe_2O_3 nanostructures for heavy metal ion removal: adsorption property and mechanism. Langmuir, 28 (2012) 4573–4579.
[29] C.L. Warner, W. Chouyyok, K.E. Mackie, D. Neiner, L.V. Saraf, T.C. Droubay, M.G. Warner, R.S. Addleman, Manganese doping of magnetic iron oxide nanoparticles: tailoring surface reactivity for a regenerable heavy metal sorbent. Langmuir, 28 (2012) 3931–3937.
[30] H. Bagheri, R. Daliri, A. Roostaie, A novel magnetic poly(aniline-naphthylamine) based nanocomposite for micro solid phase extraction of rhodamine B. Anal. Chim. Acta., 794 (2013) 38– 46.
[31] T. Wen, W. Zhu, C. Xue, J. Wu, Q. Han, X. Wang, X. Zhou, H. Jiang, Novel electrochemical sensing platform based on magnetic field-induced self-assembly of Fe_3O_4 @polyaniline nanoparticles for clinical detection of creatinine. Biosens. Bioelectron., 56 (2014) 180–185.
[32] M.J. Pirouz, M.H. Beyki, F. Shemirani, Anhydride functionalised calcium ferrite nanoparticles: a new selective magnetic material for enrichment of lead ions from water and food samples. Food Chem., 170 (2015) 131–137.
[33] M.M.G. Saldivar-Ramirez, C.G. Sanchez-Torres, D.A. Cortes-Hernandez, J.C. Escobedo-Bocardo, J.M. Almanza-Robles, A. Larson, P.J. Resendiz-Hernandez, I.O. Acuna-Gutierrez, Study on the efficiency of nanosized magnetite and mixed ferrites in magnetic hyperthermia. J. Mater. Sci. Mater. Med., 25 (2014) 2229–2236.
[34] M.H. Beyki, F. Shemirani, Dual application of facilely synthesized Fe_3O_4 nanoparticles: fast reduction of nitro compound and preparation of magnetic polyphenylthiourea nanocomposite for efficient adsorption of lead ions. RSC Adv., 5 (2015) 22224–22233.
[35] M. Baghayeri, E.N. Zare, M.M. Lakouraj, A simple hydrogen peroxide biosensor based on a novel electro-magnetic poly(p-phenylenediamine) @Fe_3O_4 nanocomposite. Biosens. Bioelectron., 55 (2014) 259–265.
[36] H. Bagheri, A. Afkhami, M. Saber-Tehrani, H. Khoshsafar, Preparation and characterization of magnetic nanocomposite of schiff base/silica/magnetite as a preconcentration phase for the trace determination of heavy metal ions in water, food and biological samples using atomic absorption spectrometry. Talanta, 97 (2012) 87–95.
[37] M.R. Huang, H.J. Lu, X.G. Li, Efficient multicyclic sorption and desorption of lead ions on facilely pre-pared poly(m-phenylenediamine) particles with extremely strong chemoresistance, J. Colloid Interface Sci., 313 (2007) 72–79.
[38] M.E. Khosroshahi, L. Ghazanfari, M. Tahriri, Characterisation of binary (Fe_3O_4/SiO_2) biocompatible nanocomposites as magnetic fluid. J. Exp. Nanosci., 6 (2011) 580–595.
[39] R.M. Khafagy, Synthesis, characterization, magnetic and electrical properties of the novel conductive and magnetic polyaniline/$MgFe_2O_4$ nanocomposite having the core–shell structure. J. Alloys Comp., 509 (2011) 9849–9857.
[40] L.I. Cabrera, A. Somoza, J.F. Marco, C.J. Serna, M.P. Morales, synthesis and surface modification of uniform MFe_2O_4 (M = Fe, Mn, and Co) nanoparticles with tunable sizes and functionalities. J. Nanopart. Res., 14 (2012) 873–887.
[41] X.Y. Yu, T. Luo, Y.Z. Zhang, Y. Jia, B.J. Zhu, X.C. Fu, J.H. Liu, X.J. Huang, Adsorption of lead(II) on O_2-plasma-oxidized multiwalled carbon nanotubes: thermodynamics, kinetics, and desorption. ACS Appl. Mater. Interfaces, 3 (2011) 2585–2593.
[42] J. Dai, H. Yan, H. Yang, R. Cheng, Simple method for preparation of chitosan/poly(acrylic acid) blending hydrogel beads and adsorption of copper(II) from aqueous solutions. Chem. Eng. J., 165 (2010) 240–249.
[43] J.U.K. Oubagaranadin, Z.V.P. Murthy, Adsorption of divalent lead on a montmorillonite-illite type of clay. Ind. Eng. Chem. Res., 48 (2009) 10627–10636.
[44] J.L. Gong, X.Y. Wang, G.M. Zeng, L. Chen, J.H. Deng, X.R. Zhang, Q.Y. Niu, Copper (II) removal by pectin–iron oxide magnetic nanocomposite adsorbent. Chem. Eng. J., 185–186 (2012) 100–107.
[45] L. Jiang, S. Xiao, J. Chen, Removal behavior and mechanism of Co(II) on the surface of Fe–Mn binary oxide adsorbent, Colloids Surf. A: Physicochem. Eng. Aspects, 479 (2015) 1–10.
[46] L.D. Hafshejani, S.B. Nasab, R.M. Gholami, M. Moradzadeh, Z. Izadpanah, S.B. Hafshejani, A. Bhatnagar, Removal of zinc and lead from aqueous solution by nanostructured cedar leaf ash as biosorbent, J. Mol. Liq., 211 (2015) 448–456.
[47] X. Huang, M. Pan, The highly efficient adsorption of Pb(II) on graphene oxides: A process combined by batch experiments and modeling techniques, J. Mol. Liq., 215 (2016) 410–416.
[48] S. Chowdhury, P. Saha, Adsorption thermodynamics and kinetics of malachite green onto $Ca(OH)_2$-treated fly ash. J. Environ. Eng., 137 (2011) 388–397.
[49] M. Tagliabue, D. Farrusseng, S. Valencia, S. Aguado, U. Ravon, C. Rizzo, A. Corma, C. Mirodatos, Natural gas treating by selective adsorption: Material science and chemical engineering interplay. Chem. Eng. J., 155 (2009) 553–566.
[50] T. Wakatsuki, U. Furukawa, K. Kawaguchi, Specific and non-specific adsorption of inorganic ions I. Evaluation of specific adsorbability by means of minimum concentration for specific adsorption, oil Sci, Plant Nutr., 20 (1974) 353–362.
[51] M. Bayat, F. Shemirani, M.H. Beyki, Utilization of facile synthesized Fe_3O_4 nanoparticles as a selective support for preconcentration of lead ions from food and environmental samples, Anal. Methods, 6 (2014) 5345–5352.